PHYSICAL REVIEW A VOLUME 27, NUMBER 6 JUNE 1983

Photon echoes in lithium vapor with the use of angled excitation beams

R. Beach, B. Brody,* and S. R. Hartmann
Columbia Radiation Laboratory, Department of Physics, Columbia University, New York, New York 10027
(Received 7 January 1983)

Two-pulse photon echoes on the $2^2S_{1/2}$-$2^2P_{3/2}$ transition in lithium vapor are generated using laser excitation pulses with angular separations of 0.70 and 1.40 mrad. The observed degradation of echo intensity with angling of the excitation pulses is in agreement with theory. The largest echoes radiated by the lithium sample contained 10^9 photons; the smallest echoes detected contained only an average of 0.04 photons. This intensity range of greater than 10^{10} represents measurements made over more than 15 natural lifetimes of the $2^2P_{3/2}$ state despite the degradation due to angling. Modulation of the echo signal due to the hyperfine structure of the $2^2P_{3/2}$ state is also observed.

INTRODUCTION

The very first photon-echo experiment, in ruby, used angled excitation beams in order to protect the echo detecting photomultiplier from saturation by the relatively intense excitation pulses.[1] Excitation pulses at $t=0$ and $t=\tau$ with nonparallel wave vectors $\vec{k}_1$ and $\vec{k}_2$ produce a polarization density with wave vector $\vec{k}_{\text{echo}}=2\vec{k}_2-\vec{k}_1$, which radiates an echo at $t=2\tau$. If the angle θ between $\vec{k}_1$ and $\vec{k}_2$ is small then $\vec{k}_{\text{echo}}$ is shifted 2θ from $\vec{k}_1$. For θ larger than the beam divergence of either excitation pulse it is possible to use an aperture stop to block the excitation pulses and allow only the echo signal to enter the optical detection apparatus.

A disadvantage of this technique is that the magnitude of $\vec{k}_{\text{echo}}$ differs from $k=|\vec{k}_1|=|\vec{k}_2|$ by the amount $\Delta k=k\theta^2$. In order for constructive interference to occur throughout a sample of length L we must have $L\,\Delta k<1$ and consequently $\theta<(Lk)^{-1/2}$. But $(Lk)^{-1/2}$ is just the beam divergence of a small Fresnel number sample. For such a sample it is therefore not possible to separate the echo from the excitation pulses using an angled beam technique without degrading the echo. For a large Fresnel number sample the beam divergence is $(Dk)^{-1}$, where D is the transverse dimension of the sample and $(Dk)^{-1}\ll(Lk)^{-1/2}$. For such samples it is a simple matter to have the echo radiated outside the beam divergence of the excitation pulses.

Pockels cell shutters and acousto-optic modulators (AOM) respond fast enough to allow an echo to be observed while still protecting a photomultiplier detector from the intense excitation pulses when working with pulse separations on the order of tens of nanoseconds or more. For picosecond pulses with picosecond pulse separation techniques such as beam angling which inherently provide photomultiplier protection are needed. Another such method is the backward wave echo which uses angled beams in a three-pulse or stimulated echo configuration to produce a separated echo.[2,3] This method has the advantage that phase matching is perfect. However, imperfect phase matching may not be a serious disadvantage as long as it allows sufficient separation of the echo and excitation beams without seriously degrading the echo. Picosecond experiments have in fact been reported which successfully use angled excitation beams in a simple two-pulse configuration.[4]

Independently of whether "perfect" phase matching is possible there is a limit for experiments done in gaseous samples beyond which neither of the above techniques yields results which are independent of the angle between the excitation beams. This is best seen by applying the billiard-ball echo model[5] to the two-pulse echo with angled excitation beams. The first pulse at $t=0$ produces an excited-state wave packet which recoils from the original ground-state wave packet with velocity $\vec{v}=\hbar\vec{k}_1/m$. We show this excited state trajectory by the dotted line from the origin in Fig. 1 where the wave vector $\vec{k}_1$ is directed along the x axis and time is measured along the axis to the right. The ground-state wave packet remains in place: Its trajectory is a line along the time axis. At $t=\tau$ the pulse with wave vector $\vec{k}_2$ is applied. This wave vector has a small component along the y axis. The pulse at τ generates new ground-state and excited-state wave packets from the stimulated emission of a photon and the absorption of a photon, respectively. The corresponding trajectories are indicated by the solid and

dashed lines which originate at $t=\tau$. If $\vec{k}_1$ and $\vec{k}_2$ had been parallel the trajectories would intersect at $t=2\tau$. With angled beams the time $t=2\tau$ is still special as this is the time when the wave packets are closest together. Calling $F_1(\vec{r})$ and $F_2(\vec{r})$ the wave-packet amplitudes of the colliding ground and excited states, respectively, the radiated electric field is proportional to[6]

$$\int d\vec{r}\, F_1\left[\vec{r}-\frac{\hbar\vec{k}_1}{m}t+\frac{\hbar\vec{k}_2}{m}(t-\tau)\right]F_2^*\left[\vec{r}-\frac{\hbar\vec{k}_2}{m}(t-\tau)\right]=\exp\left[-\left[\frac{q_0\hbar k\theta}{m}\right]^2(t-\tau)^2\right]G(t-2\tau)\,, \tag{1}$$

where $q_0=(2mk_BT/\hbar^2)^{1/2}$, θ is the angle between $\vec{k}_1$ and $\vec{k}_2$, and $G(t-2\tau)$ is a function that is independent of θ and peaked at $t=2\tau$. The exponential factor on the right-hand side of Eq. (1) demonstrates how the echo degrades with increasing θ.

This degradation of echo intensity with beam angling may be undesirable in as much as it limits the maximum τ for which one can observe echoes. On the other hand it affords a means of determining the parameter q_0 which characterizes the atomic velocity distribution. This may be of interest for monitoring a transient velocity distribution.

In an effort to determine the dynamic range of echo intensities which can be readily observed we have performed a simple two-pulse echo experiment in lithium vapor using angled excitation beams. With angled beams we can see echoes for small τ, without limitation from slow optical shutters. For longer τ and smaller echoes we use an AOM to provide photomultiplier protection, which enables us to measure very weak echoes by photon counting. Echoes are obtained at two different beam angles, which enables us to cancel out the effects of quantum beats and atomic lifetime echo signal decay.

EXPERIMENT

Figure 2 presents our experimental system. Two Littman-cavity pulsed dye lasers (DL), pumped by a pair of Quanta-Ray DCR-1A Nd:YAG (yttrium aluminum garnet) lasers, were tuned to 6708 Å, the $2^2S_{1/2}$-$2^2P_{3/2}$ transition in lithium. A homemade external trigger circuit fired the two YAG lasers sequentially for specified pulse separations from the dye lasers. The output of each dye laser was amplified once in a transversely pumped flowing-dye cell. The dye laser output as viewed on a 6-GHz FSR etalon consisted of three cavity modes giving a total linewidth of approximately 1.5 GHz. The halfwidth at half maximum of the dye laser pulse was approximately 3 nsec. The two amplified dye laser outputs were combined, expanded, and collimated (with beam combiner BC) with an angle θ between their wave vectors. Figure 3 presents the timing sequence and angling of the excitation pulses. The combined laser beams were sent into a heat pipe containing atomic lithium vapor at a temperature of 543 K as measured by thermocouples strapped to the outside of the stainless-steel pipe which contained the lithium. The lithium vapor in the heat pipe was confined to a region that was approximately 40 cm long and 2 cm in diameter. The output pulses leaving the heat pipe (pulse 1, pulse 2, and the echo) were

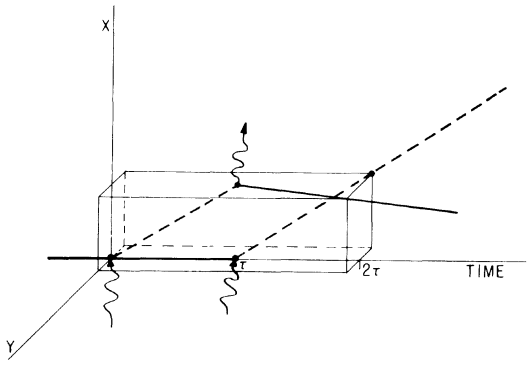

FIG. 1. Kinematics of a two-pulse echo using angled beams. The ground- and excited-state trajectories are denoted by solid and dashed lines, respectively.

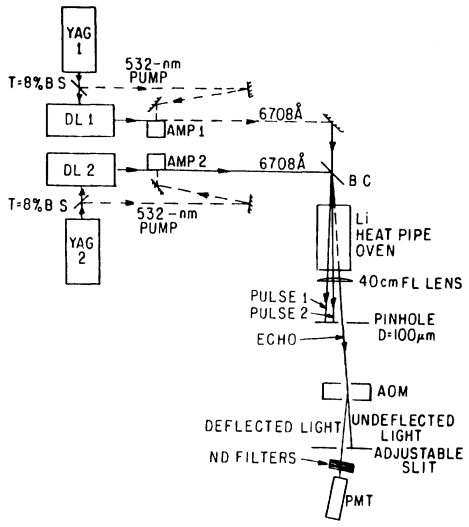

FIG. 2. Schematic diagram of our experimental setup. Here BS stands for beam splitter, and T is the transmitted intensity.

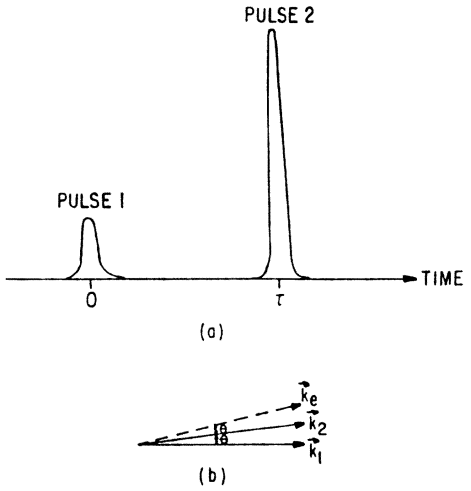

FIG. 3. (a) Timing sequence for pulse 1, a $\pi/2$ pulse, and pulse 2, a π pulse, in our experiment. (b) The angles between the wave vectors of pulse 1, pulse 2, and the photon echo.

brought to a focus in the focal plane of a lens with a focal length (FL) of 40 cm. A pinhole having a diameter of 100 μm was placed in the focal plane of this lens and positioned laterally to pass the echo signal while blocking pulses 1 and 2. This method of separating the echo signal from the excitation pulses becomes possible with angled excitation beams because the echo signal is emitted in direction $\vec{k}_{\text{echo}}$ different from the excitation pulses,[1]

$$\vec{k}_{\text{echo}}=2\vec{k}_2-\vec{k}_1 , \tag{2}$$

where $\vec{k}_1$ and $\vec{k}_2$ are the wave vectors of pulse 1 and pulse 2, respectively, as shown in Fig. 3(b). We gathered data for angular pulse separations of 0.70 ± 0.06 and 1.40 ± 0.06 mrad, corresponding to spot separations in the focal plane of the 40-cm lens of 280 and 550 μm, respectively, between both pulses 1 and 2 and pulse 2 and the echo.

Since some diffracted and scattered light from pulses 1 and 2 did leak through the pinhole an acousto-optic modulator was inserted after the pinhole to further reduce incident pulse leakage into the photomultiplier tube (PMT). The acousto-optic modulator was gated to deflect the echo signal through a slit in a screen. Past the screen the echo traversed calibrated neutral density filters (ND) and then entered our photomultiplier tube, a Varian model VPM-152M. The output of the photomultiplier was sent to a gated integrator whose output was digitized by an analog-to-digital converter for recording by a computer.

RESULTS

In both runs the pulse separation was increased in steps of 10 nsec from zero until an echo signal could no longer be detected even after averaging 200 laser shots. The echo intensity versus the time between laser pulse 1 and the echo is plotted for the two runs made at angular pulse separations of 0.70 and 1.40 mrad in Fig. 4. The large-scale modulation evident in both runs results from the hyperfine splitting of the $2^2S_{1/2}$ and $2^2P_{3/2}$ states of lithium. The modulation is a quantum beating interference among the excitable transitions.

Reference 6 gives the photon echo intensity for a two-level system as a function of the excitation pulse time separation τ and angle separation θ;

$$I_{\text{echo}}(\tau,\theta)=I_0\exp\left[-2\left[\hbar k q_0\frac{\theta}{m}\right]^2\tau^2\right]\times\exp\left[-\frac{2\tau}{T_{\text{LT}}}\right], \tag{3}$$

where T_{LT} is the excited-state lifetime.

Equation (3) is developed for two-level systems. To include the quantum beating effects of the hyperfine structure of lithium we should include in Eq. (3) a factor that depends only on the pulse separation τ. If we call this modulation factor $M(\tau)$ Eq.

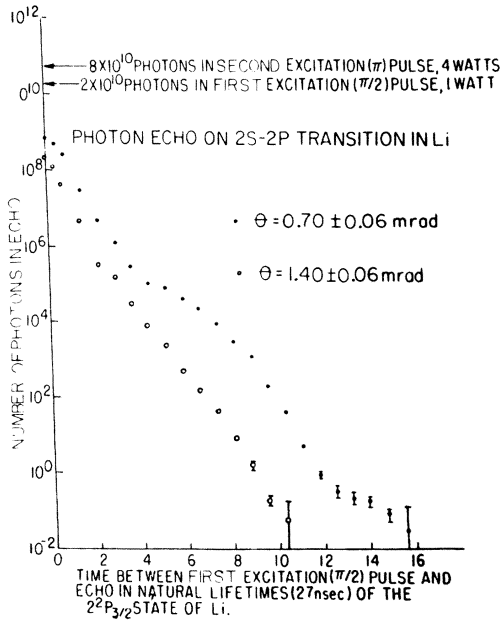

FIG. 4. Number of photons in the echo vs the time between pulse 1 and the echo in units of the natural lifetime of the $2^2P_{3/2}$ state of lithium. The angle between pulse 1 and pulse 2 is 0.70 ± 0.06 mrad in one run and 1.40 ± 0.06 mrad in the other run.

(3) for the echo intensity becomes

$$I_{\text{echo}}(\tau,\theta)=I_0\exp\left[-2\left[\frac{\hbar k q_0\theta}{m}\right]^2\tau^2\right]\times\exp\left[-\frac{2\tau}{T_{\text{LT}}}\right]M(\tau)\,. \tag{4}$$

To check Eq. (3) we have plotted in Fig. 5 the ratio of the echo signals for the two angles plotted separately in Fig. 4. Data from two other runs at these same two angles are included in Fig. 5. Finally, the solid curve in Fig. 5 is the prediction of Eq. (3) for this ratio,

$$R(\tau)=\frac{I_{\text{echo}}(\tau,\theta_1=1.4\text{ mrad})}{I_{\text{echo}}(\tau,\theta_2=0.7\text{ mrad})}=R_0\exp\left[-2\left[\frac{\hbar k q_0}{m}\right]^2(\theta_1^2-\theta_2^2)\tau^2\right]\,. \tag{5}$$

In our experiment

$$R(\tau)=R_0e^{-(\tau/\tau_{\text{eff}})^2} \tag{6}$$

with

$$\tau_{\text{eff}}=55\text{ nsec}\,. \tag{7}$$

Analyzing the data in this fashion facilitates comparison with the predictions of Eq. (3) for the degradation of the echo signal with angling the beams since the modulation of the echo signal and the lifetime decay cancel out of the ratio $R(\tau)$. The data and the calculated curve in Fig. 5 are in good agreement.

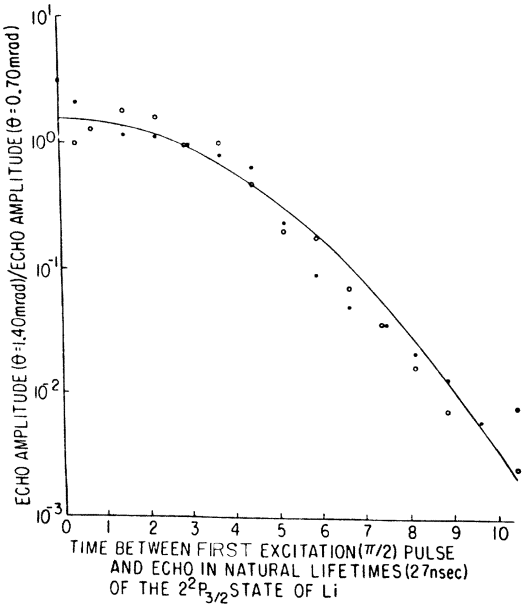

FIG. 5. Ratio of the echo signals for the two angles plotted separately in Fig. 4 (solid dots). This ratio for data at the same two angles, taken in an independent run, is also shown (open dots). The solid line is the prediction of Eq. (3) for this ratio as given by Eq. (5).

The error bars in Fig. 4 represent fluctuations in the number of photons we detected in the echo at a given τ. There is another source of uncertainty in our data that is not indicated. In Fig. 4 we have pieced together data taken with neutral density filters ranging from ND0 to ND6: The error bars shown do not include this uncertainty in the calibration of these filters.

The angled beam technique makes it possible to look at echoes at short pulse separations without using optical shutters. Since the echoes produced at small τ are large, photodiodes can be used for their detection. With an EG&G FND-100 silicon photodiode mounted in front of the photomultiplier we measured the echo intensity for $\tau=5$ nsec. We then centered the pinhole to pass excitation pulse 2 and measured its amplitude. Using the manufacturer's quoted spectral response[7] we inferred the echo and pulse 2 to contain roughly 10^9 photons and 10^{11} photons, respectively. Thus echoes can readily be generated which are comparable in amplitude—within a factor of 10—100—to the excitation pulses which generated them. These large echoes are visible to the unaided eye and can be used to optimize alignment of the apparatus. The smallest echoes detected contained an average of only a small fraction of a photon per echo and required photon counting techniques. The maximum time to accumulate a photon counting datum was 20 sec: We were able to detect roughly one photon in every 25 echoes, or an average of 0.04 photons per echo.

CONCLUSION

Our experiment verified the expected dependence of echo intensity on angling of the excitation pulses while demonstrating the large dynamic range over which echo signals can be observed. Our data taken at 0.70 ± 0.06 mrad ranged in intensity over almost 11 orders of magnitude. Experiments covering even larger dynamic ranges are being planned.

For a sample of echo atoms one absorption length long we observed that the largest echo was within a factor of 100 of the amplitude of the π excitation pulse. This is a general result: the number of photons in the largest echo always scales with the number of photons in the excitation pulse.[8] Paradoxically, since the excitation pulse area depends on the square root of the pulse intensity times the resonant oscillator strength, a system with a smaller oscillator

strength calls for more incident excitation photons and will therefore give larger echoes.

ACKNOWLEDGMENTS

We would like to thank R. Kichinski, T. J. Chen, E. Xu, and E. Whittaker for help in some phases of the experiment, M. Glick for help in acquiring some of the data, and Rita Mahon and Frank Tompkins for the design of our dye-laser oscillator amplifier system. This work was supported by the Joint Services Electronics Program (U.S. Army, U.S. Navy, and U.S. Air Force) under Contract Nos. DAAG29-79-C-0079 and DAAG29-82-K-0080 and by the Office of Naval Research under Contract No. N00014-78-C-0517.

---

*Permanent address: Bard College, Annandale-on-Hudson, N.Y. 12504.

[1]I. D. Abella, N. A. Kurnit, and S. R. Hartmann, Phys. Rev. 141, 391 (1966).

[2]M. Fujita, H. Nakatsuka, H. Nakanishi, and M. Matsuoka, Phys. Rev. Lett. 42, 974 (1979).

[3]T. Mossberg, A. Flusberg, and S. R. Hartmann, Phys. Rev. Lett. 42, 1665 (1979).

[4]P. Hu and H. M. Gibbs, J. Opt. Soc. Am. 68, 1631 (1978).

[5]R. Beach, S. R. Hartmann, and R. Freidberg, Phys. Rev. A 25, 2658 (1982).

[6]R. Beach, B. Brody, and S. R. Hartmann, Phys. Rev. A 27, 2537 (1983).

[7]EG&G, Electro-Optics Division, Data Sheet D3013B-1.

[8]T. W. Mossberg, R. Kachru, and S. R. Hartmann, Phys. Rev. A 20, 1976 (1979).